doi:10.1038/nature12030

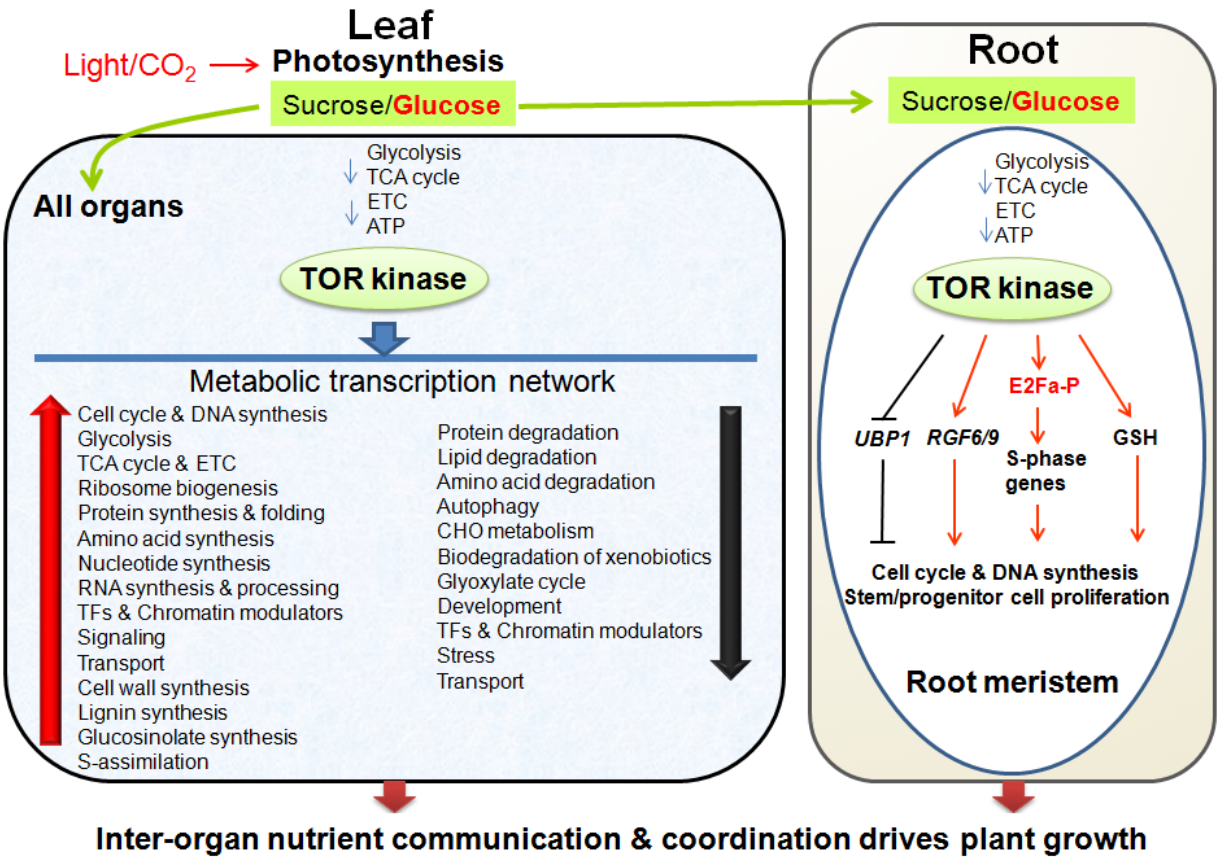

Supplementary Figure 1 | Glucose-TOR transcription networks mediate inter-organ dialogues to drive plant growth. Leaf photosynthesis produces sucrose and glucose to fuel plant growth. Glucose activates TOR kinase via glycolysis and mitochondrial bioenergetic relays to orchestrate global transcriptional reprogramming, which integrates central and secondary carbon metabolism with bioenergetics, biosynthesis, signalling, TFs, chromatin modulators, transporters, autophagy, and cell cycle regulation. Significantly, glucose-TOR signalling is integrated in local promotion of root meristem activation by transcriptional regulation of genes for cell cycle entry, root growth factors (*RGF*), *UPBEAT1*(*UPB1*) transcription factor and glutathione (GSH) synthesis via inter-organ coordination. ETC, electron transport chain.

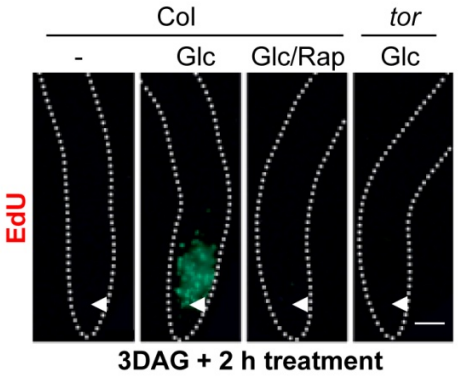

Supplementary Figure 2 | Rapid reactivation of the quiescent root meristem. Cell cycle re-entry is quickly reactivated by 2 h of glucose (Glc, 15 mM) treatment in seedlings 3 DAG, but is blocked by rapamycin (Rap) or in the *tor* mutant. S-phase entry is visualized by EdU *in situ* staining. Scale bar: 50 µm.

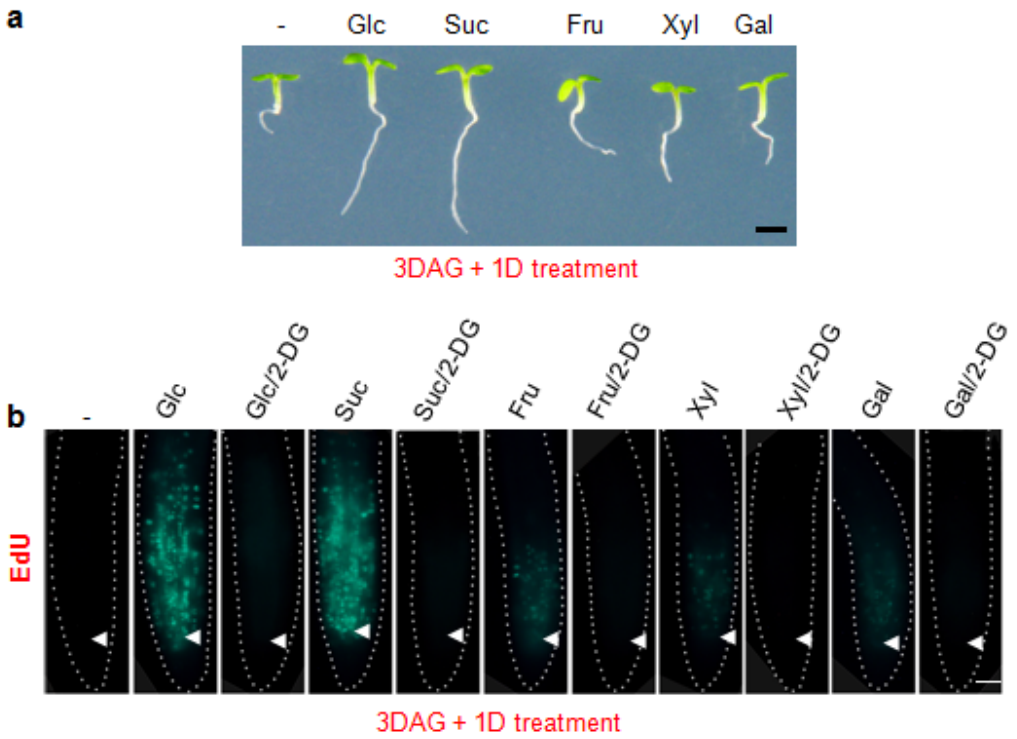

Supplementary Figure 3 | Differential sugar effects on root growth and meristem activation. **a,** Root growth activation by different sugars. **b,** Quiescent root meristem activation by different sugars. Sugars (15 mM) were added to seedlings grown in liquid medium at 3DAG for 24 h. Glucose (Glc), sucrose (Suc), fructose (Fru), xylose (Xyl) and galactose (Gal) were examined. Meristem activation was blocked by 2-DG (2-Deoxyglucose), a glycolysis inhibitor. Scale bar, 1 mm or 25 µm.

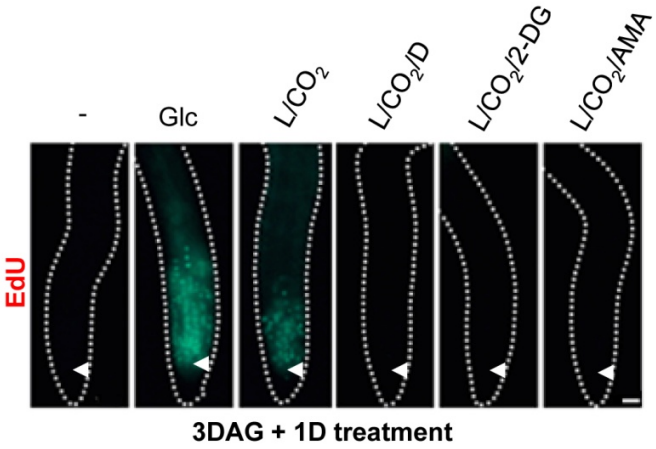

Supplementary Figure 4 | Reactivation of the quiescent root meristem by photosynthesis requires glycolysis and mitochondrial bioenergetic relays. Quiescent root meristem cells were reactivated by 24 h of enhanced photosynthesis (200 µmol/m^2 s light in 400 µl liquid medium, 0.5 x MS and 6 mM Na_2CO_3, pH 5.7), which was prevented by inhibitors targeting photosynthesis, glycolysis or mitochondria. Glucose (Glc, 15 mM), light (L), DCMU (D, 20 µM), 2-Deoxyglucose (2-DG, 10 mM), and antimycin A (AMA, 5 uM). Scale bar: 25 µm.

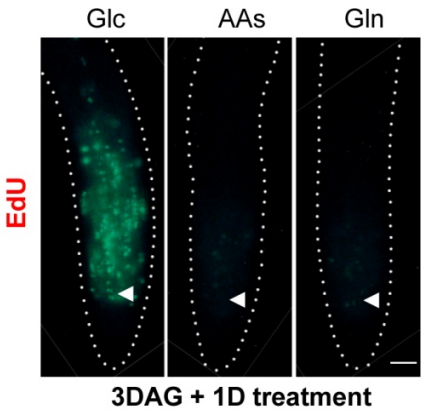

Supplementary Figure 5 | Amino acids cannot activate the quiescent root meristem. The quiescent root meristem was treated with glucose (Glc, 15 mM), amino acid mix (AAs, 0.1 mM each for 17 amino acids) or glutamine (Gln, 0.1 mM) for 24 h. Up to 1 mM each for the 17-amino-acid mix and up to 5 mM Gln did not activate the quiescent root meristem. S-phase entry is visualized by EdU in situ staining. Scale bar: 25 μm.

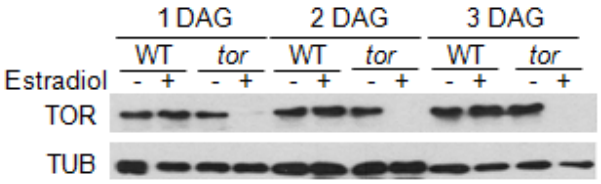

Supplementary Figure 6 | Time-course analysis of TOR expression in the inducible *tor* mutant. Estradiol treatment (10 μM) triggered quick degradation of TOR proteins in the inducible *tor* mutants. DAG, day after germination.

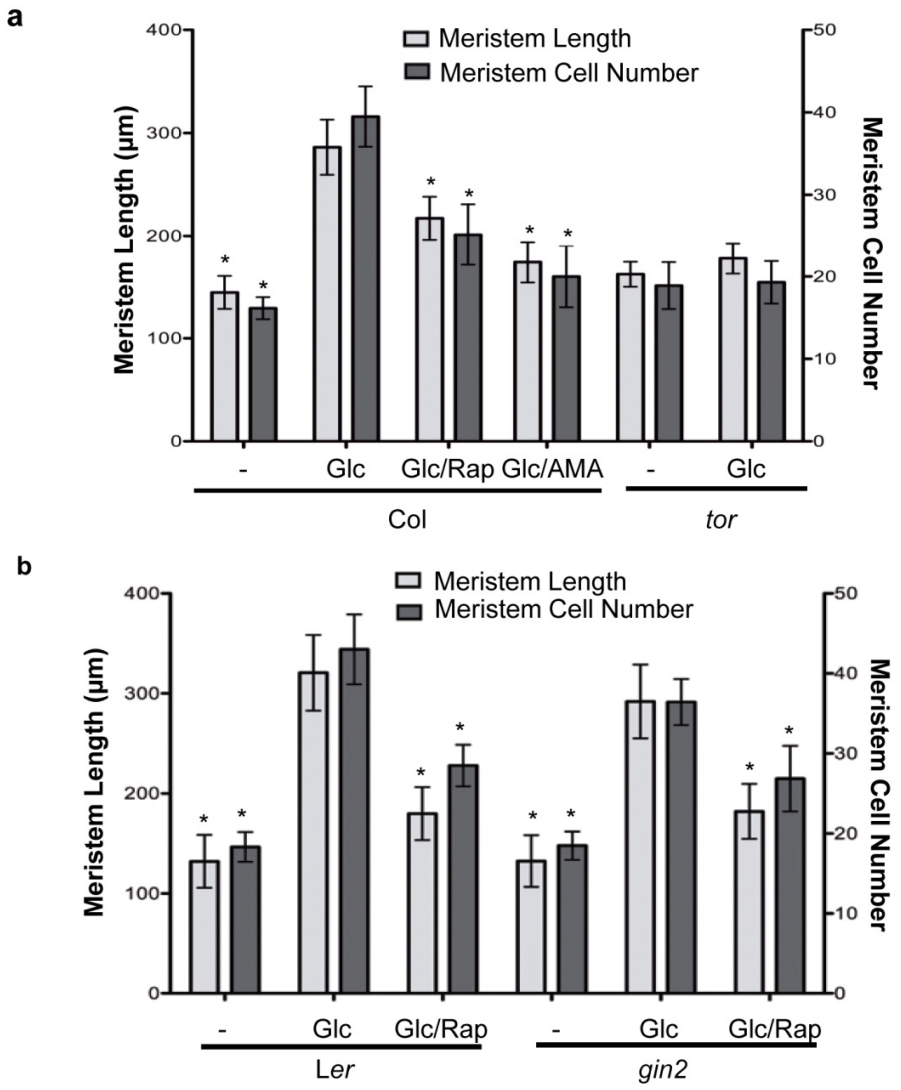

Supplementary Figure 7 | Glucose-TOR signalling promotes root meristem activation. a, b, Quantitative measurement of root meristem length and cell number in 3DAG WT (Col or L*er*), *tor* and *gin2* seedlings after 24 h treatment without or with glucose (Glc), and without or with rapamycin (Rap, 10 µM) or AMA (5 µM). For *tor* seedlings, estradiol (10 µM) was added at the beginning of germination. Values represent means; error bars are s.d. (n>30). Unpaired Student's t test was used to identify significant differences (**P*<0.05) when compared with the data from samples treated with glucose.

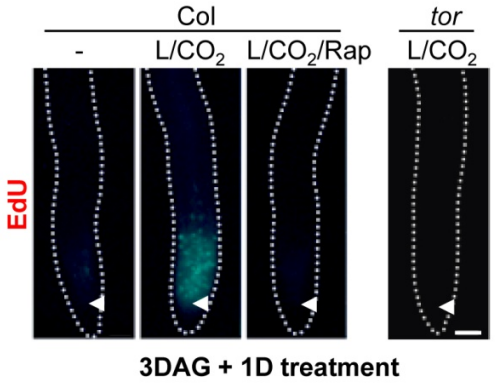

Supplementary Figure 8 | Reactivation of the quiescent root meristem by photosynthesis requires TOR signalling. Quiescent root meristem cells were reactivated by 24 h of enhanced photosynthesis (200 µmol/m^2 s light in 400 µl liquid medium, 0.5 x MS and 6 mM Na_2CO_3, pH 5.7), which was blocked by rapamycin (Rap, 10 µM) or in the *tor* mutant. Scale bar: 50 µm.

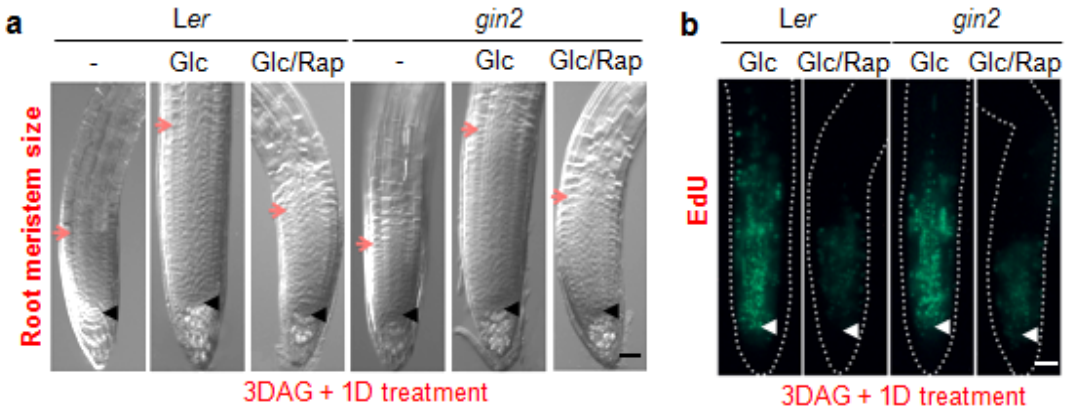

Supplementary Figure 9 | TOR kinase but not glucose sensor (*gin2*) controls root meristem activation and S-phase entry. Glucose (Glc, 15 mM); Rapamycin (Rap, 10 μM). Scale bar, 25 μm.

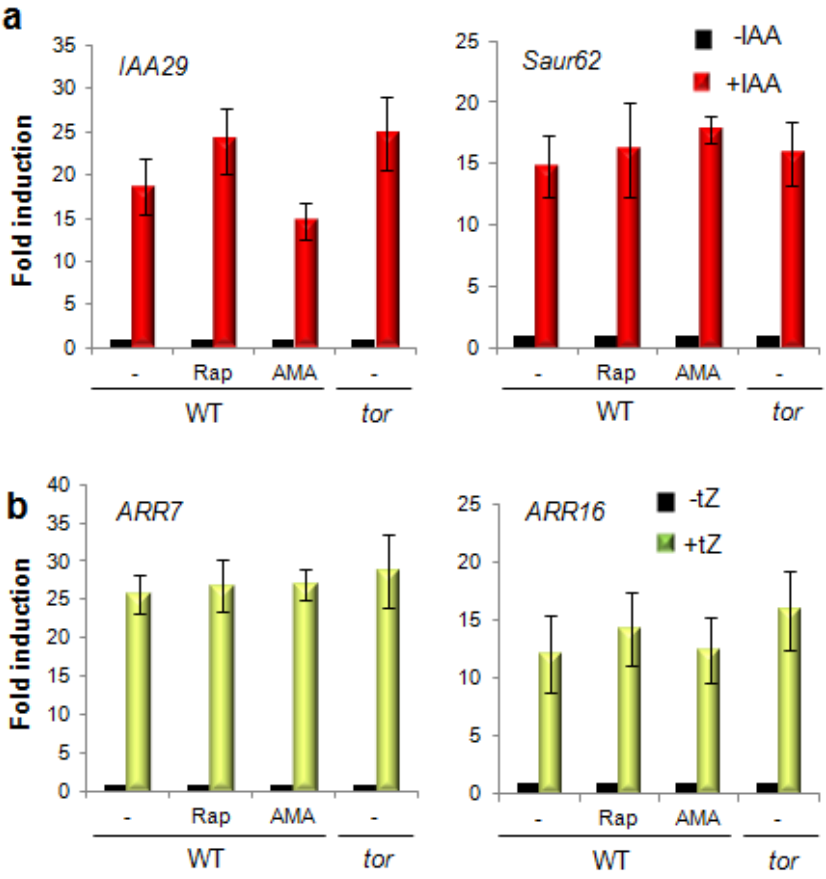

Supplementary Figure 10 | Rapamycin, AMA and tor do not interfere cytokinin and auxin signalling. a, Auxin signalling does not require TOR signalling and mitochondrial energy relay. **b**, Cytokinin signalling does not require TOR signalling and mitochondrial energy relay. Primary auxin and cytokinin marker genes were activated by 1h of indole-3-acetic acid (IAA) or trans-Zeatin (tZ) treatment in seedlings at 3DAG, and analysed by quantitative RT-PCR. Error bars are s.d., n=3. *IAA29*: *INDOLE-ACIDIC ACID29*; *Saur62*: *Small-Auxin-Up-Regulated62*; *ARR7*: *Arabidopsis Response Regulator7*; *ARR16*: *Arabidopsis Response Regulator16*.

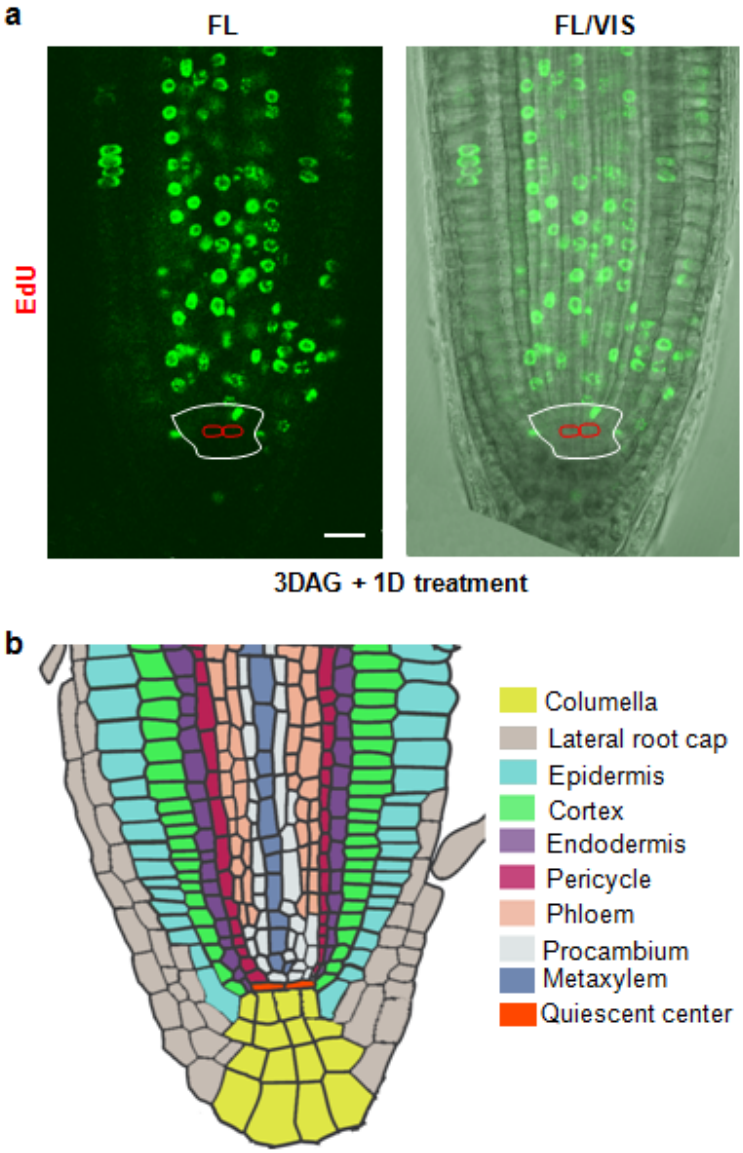

Supplementary Figure 11 | Glucose-TOR signalling activates the cell cycle in stem and progenitor cells in the root meristem. a, Reactivation of the quiescent root meristem by 24 h glucose treatment. S-phase entry is visualized by EdU staining. Red circles indicate quiescent-centre cells and the white outline marks the stem cell initials. Scale bar: 10 µm. **b,** A schematic diagram representing cell types in *Arabidopsis* root meristem. EdU staining was observed in all cell types in the root meristem after glucose stimulation, except the quiescent centre.

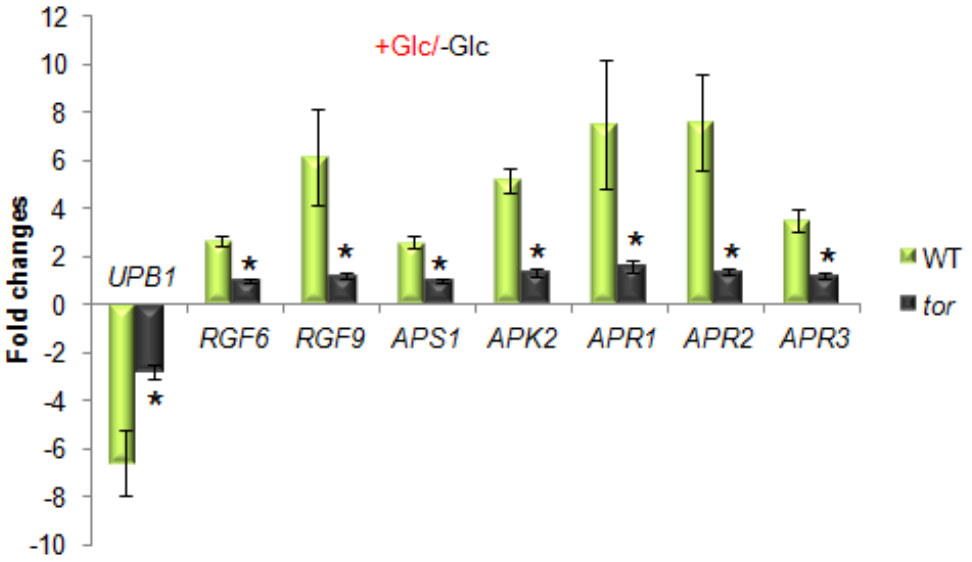

Supplementary Figure 12 | Glucose-TOR signalling controls the expression of *UPB1, RGF* and S-assimilation genes. Glucose activates genes for root growth factors (*RGF*) and S-assimilation but inhibits the gene encoding UPBEAT (*UPB1)* transcription factor in WT but not in the *tor* mutant. *RGF6, At4g16515*; *RGF9, At5g64770*; *APS1* (*At3g22890*), ATP sulfurylase1; *APK2* (*At4g39940*), APS kinase 2; *APR1* (*At4g04610*), Adenosine-5'-phosphosulfate reductase1; *APR2*, *At1g62180*; *APR3*, *At4g21990*. Results are means from ATH1 GeneChip analyses. Error bars are s.d. (n=3). Unpaired Student's t test was used to identify significant differences (*P<0.05) when compared with the data from WT samples treated with glucose.

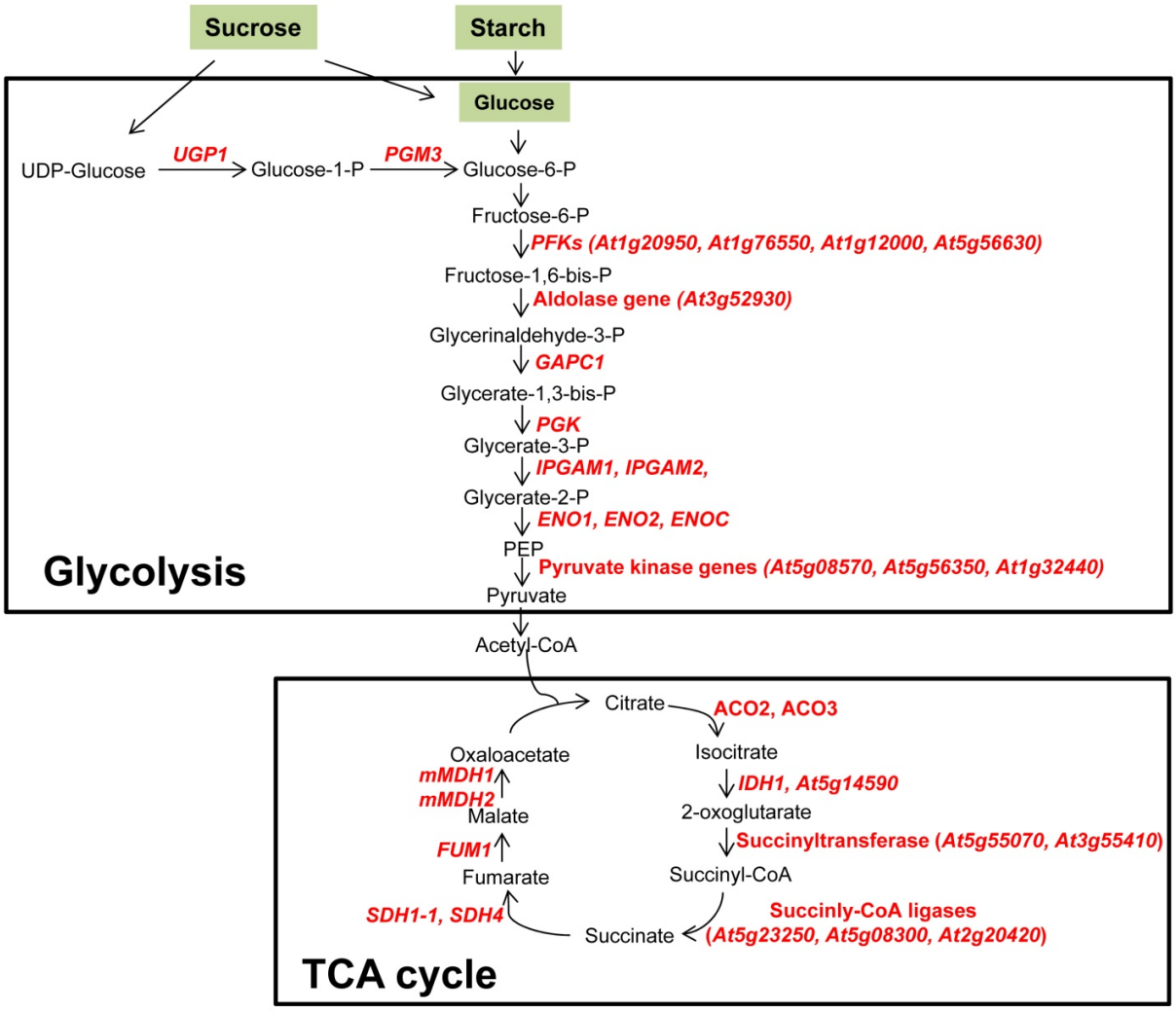

Supplementary Figure 13 | Glucose-TOR signalling activates transcript levels of glycolysis and TCA cycle genes. Simplified schemes for the sucrose and starch metabolism pathways based on Mapman[1]. Genes with elevated transcript levels in glucose-TOR signalling are highlighted by red letters (see Supplementary Table 1, 5 for details). Sucrose and starch are hydrolysed to glucose. Pyruvate is generated via glycolysis and converted to acetyl-CoA to enter the TCA (tricarboxylic acid) cycle in the mitochondria. *UGP1* (*At3g03250*), UDP-glucose pyrophosphorylase1; *PGM3* (*At1g23190*), phosphoglucomutase3; *PFK*, phosphofructokinase; *GAPC1* (*At3g04120*), glyceraldehydes-3-phosphate dehydrogenase C; *PGK* (*At1g79550*), phosphoglycerate kinase; *IPGAM1* (*At1g09780*), 2,3- biphosphoglycerate-independent phosphoglycerate mutase 1; *IPGAM2* (*At3g08590*), 2,3- biphosphoglycerate-independent phosphoglycerate mutase 2; *ENO1* (*At1g74030*), enolase 1; *ENO2* (*At2g36530*), enolase 2; *ENOC* (*At2g29560*), enoloase C; *ACO2* (*At4g26970*), aconitase 3; *ACO3* (*At2g05710*), aconitase 3; *IDH1* (*At4g35260*), isocitrate dehydrogenase 1; *SDH1-1* (*At5g66760*), succinate dehydrogenase 1-1; *SDH4* (*At2g46505*), succinate dehydrogenase 4; *FUM1* (*At2g47510*), fumarase 1; *mMDH1* (*At1g53240*), mitochondrial malate dehydrogenase 1, *mMDH2* (*At3g15020*), mitochondrial malate dehydrogenase 2.

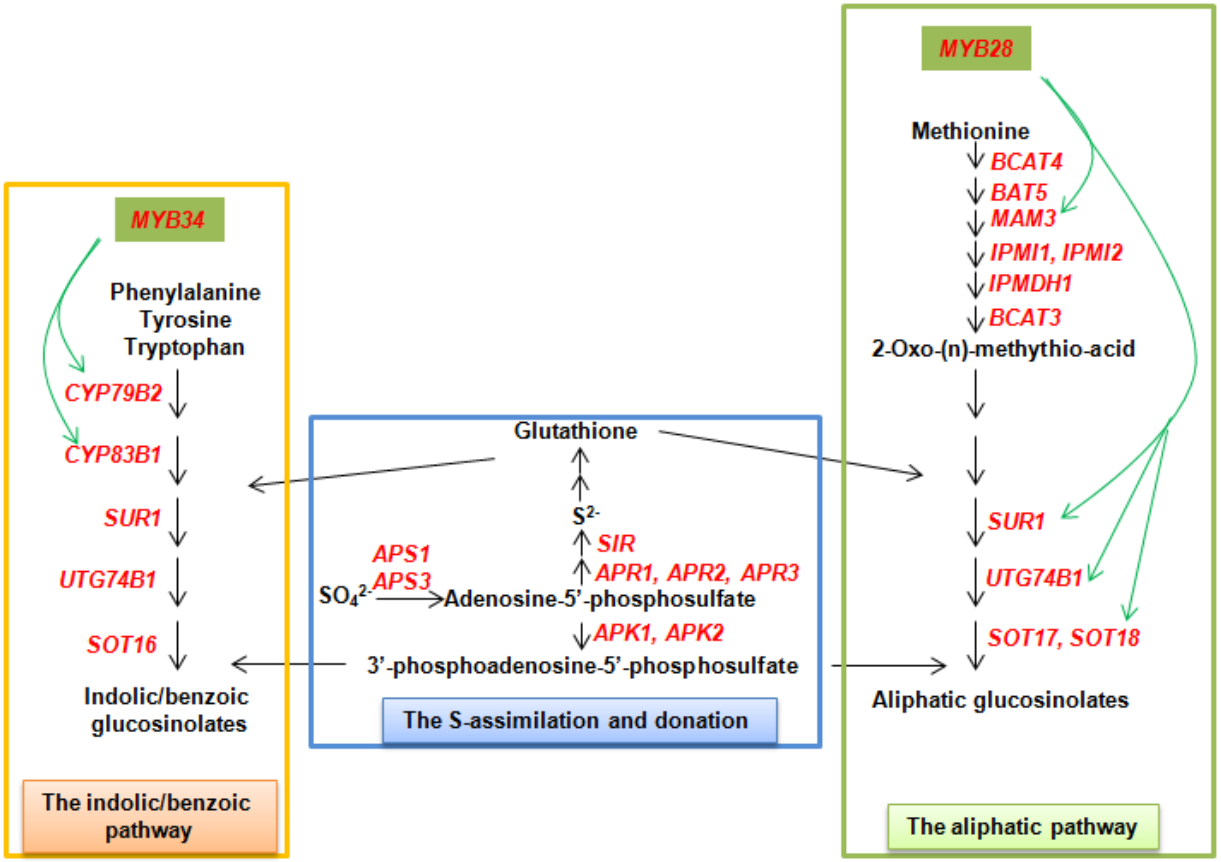

Supplementary Figure 14 | Glucose-TOR signalling activates transcript levels of genes involved in glucosinolate synthesis and S-assimilation. Simplified diagrams of the glucosinolate synthetic pathway and S-assimilation pathway, which provide the co-substrates glutathione and PAPS (3'-phosphoadenosine-5'-phosphosulfate), are shown. Genes with elevated transcript levels in glucose-TOR signalling are highlighted by red letters (see Supplementary Table 1, 5 for details). *MYB34* (*At5g60890*), MYB34 transcription factor; *MYB28* (*At5g61420*); *SUR1* (*At2g20610*), superroot1; *CYP79B2* (*At4g39950*), cytochrome P450 79B2; *CYP83B1* (*At4g31500*), cytochrome P450 83B1; *UGT74B1* (*At1g24100*), UDP-glucosyltransferase 74B1; *SOT16* (*At1g74100*), sulfotransferase 16; *SOT17* (*At1g18590*), sulfotransferase 17; *SOT18* (*At1g74090*), sulfotransferase 18; *BCAT4* (*At3g19710*), branched-chain aminotransferase 4; *BAT5* (*At4g12030*), bile acid transporter 5; *MAM3* (*At5g23020*), methythioalkymalate synthase-like 3; *IPMI1* (*At3g58990*), isopropylmalate isomerase 1; *IPMI2* (*At2g43100*), isopropylmalate isomerase 2; *IPMDH1* (*At1g31180*), isopropylmalate dehydrogenase 1; *BCAT3* (*At3g49680*), branched-chain aminotransferase 3; *APS1* (*At3g22890*), ATP sulfurylase 1; *APS3* (*At4g14680*), ATP sulfurylase 3; *APK1* (*At2g14750*), APS kinase 1; *APK2* (*At4g39940*), APS kinase 2; *APR1* (*At4g04610*), APS reductase 1, *APR2* (*At1g62180*), APS reductase 2; *APR3* (*At4g21990*), APS reductase 3; *SIR* (*At5g04590*), sulfite reductase. The genes controlled by MYB34 or MYB28 are indicated by green arrows.

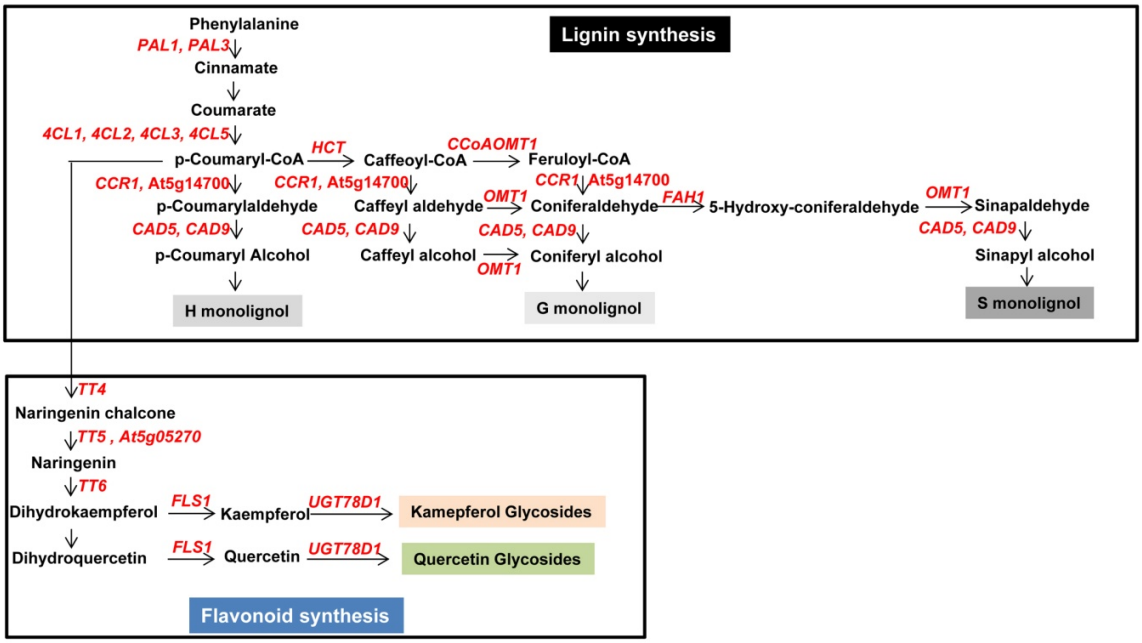

Supplementary Figure 15 | Glucose-TOR signalling activates the transcript levels of essential genes for lignin and flavonoid synthesis. Simplified schemes for monolignol and flavonoid synthetic pathways are based on Mapman[1]. Genes with elevated transcript levels in glucose-TOR signalling are highlighted by red letters (see Supplementary Table 1, 5 for details). *PAL1* (*At2g37040*), phenylalanine ammonia lyase 1; *PAL3* (*At5g04230*), phenylalanine ammonia lyase 3; *4CL1* (*At1g51680*), 4-coumarate-CoA ligase 1; *4CL2* (*At3g21240*), 4-coumarate-CoA ligase 2; *4CL3* (*At1g65060*), 4-coumarate-CoA ligase 3; *4CL5* (*At3g21230*), 4-coumarate-CoA ligase 5; *HCT* (*At5g48930*), quinate-hydroxycinnamoyl transferase; *CCoAOMT1* (*At4g34050*), caffeoyl coenzyme A O-methyltransferase 1; *CCR1* (*At1g15950*), cinnamoyl CoA reductase 1; *CAD5* (*At4g34230*), cinnamyl alcohol dehydrogenase 5; *CAD9* (*At4g39330*), cinnamyl alcohol dehydrogenase 9; *OMT1* (*At5g54160*), O-methyltransferase 1; *FAH1* (*At4g36220*), ferulic acid 5-hydroxylase 1; *TT4* (*At5g13930*), chalcone synthase; *TT5* (*At3g55120*), chalcone isomerase; *TT6* (*At3g51240*), flavanone 3-hydroxylase; *FLS1* (*At5g08640*), flavonol synthase 1; *UGT78D1* (*At1g30530*), UDP-glucosyl transferase 78D1.

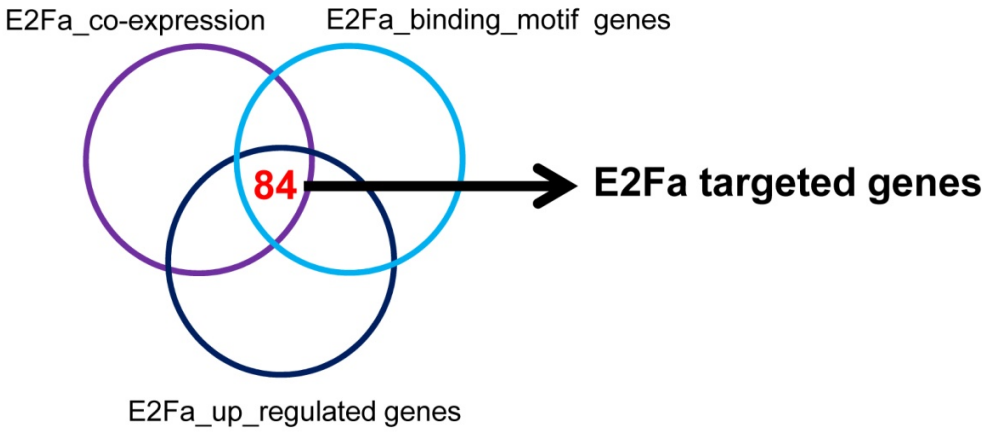

Supplementary Figure 16 | Bio-computational strategies for defining putative E2Fa target genes. *E2Fa* co-expression genes were generated by Genevestigator. E2Fa-binding motif containing genes were identified as described[2]. E2Fa up-regulated genes were identified from seedlings that ectopically express E2Fa and DPa transcription factors driven either by the 35S constitutive promoter[2,3] or the DEX-inducible promoter[4]. The genes presented in all of these three categories were defined by Venn diagram[5], and used for comparison with glucose-TOR-activated genes (Fig. 4f). See supplementary Table 7 for complete gene sets.

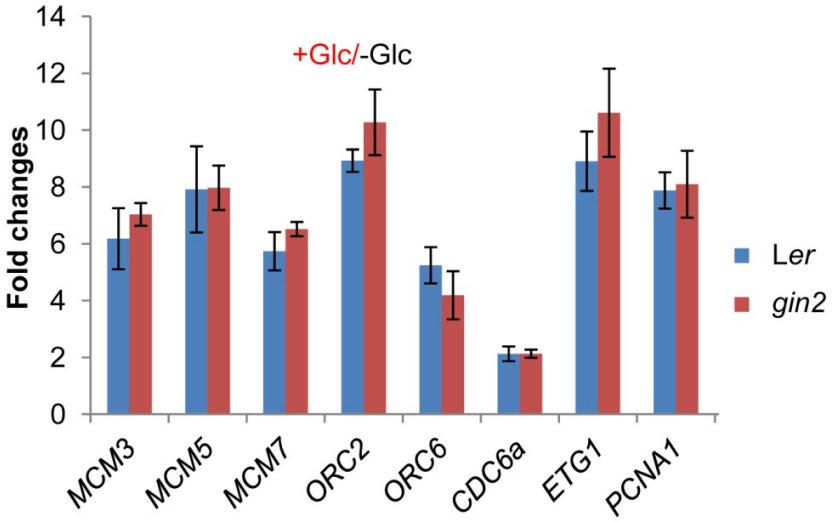

Supplementary Figure 17 | Activation of S-phase genes by glucose is independent of the HXK1-mediated signalling pathway. L*er* and *gin2* seedlings (3DAG) were treated with glucose (15 mM) for 2 h. Total RNA was isolated and quantitative RT-PCR was performed to analyse S-phase genes activation. Values represent means; error bars indicate s.d. (n=3).

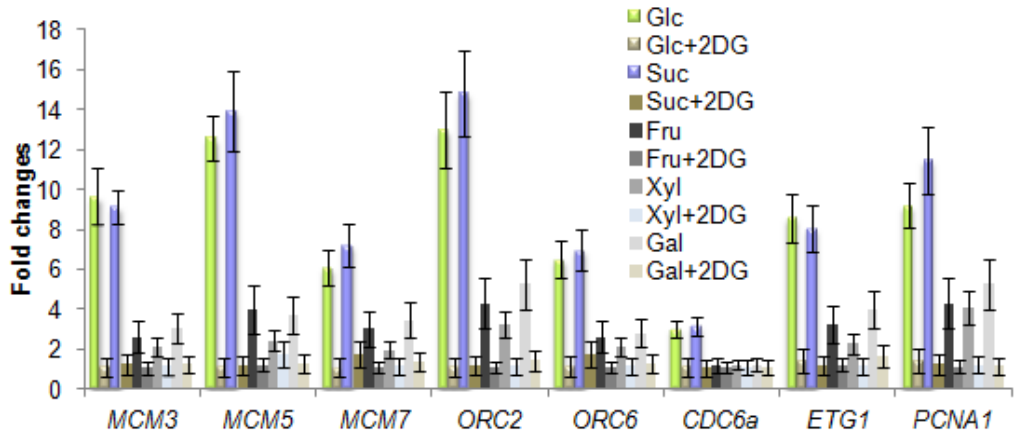

Supplementary Figure 18 | Differential sugar effects on the activation of S-phase genes. WT seedlings (3DAG) were treated with different sugars (15 mM) for 2 h. Total RNA was isolated and quantitative RT-PCR was performed to analyse S-phase genes activation. Values represent means; error bars indicate s.d. (n=3). Glucose (Glc), sucrose (Suc), fructose (Fru), xylose (Xyl) and galactose (Gal) were examined. Gene activation was blocked by 2-DG (2-Deoxyglucose), a glycolysis inhibitor.

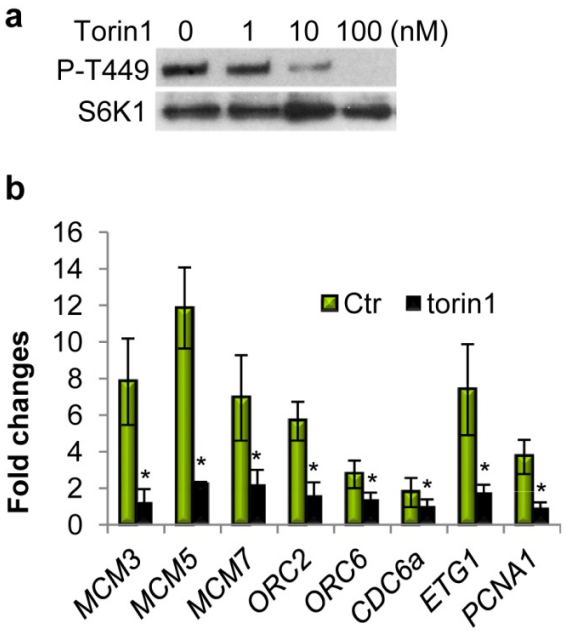

Supplementary Figure 19 | Torin1 suppresses TOR kinase activity and E2Fa activation. a, S6K1 T449 phosphorylation is inhibited by torin1. Protoplasts transiently expressing S6K1-FLAG were treated with torin1 (100 nM) for 30 min. Total proteins were analysed by protein blot analysis using anti-human-p70-phospho-T389 (P-T449) or anti-FLAG antibody (S6K1). **b,** Torin1 (100 nM) blocks S-phase gene activation by E2Fa. E2Fa-HA was transiently expressed in protoplasts for 4 h without or with torin1 treatment. Total RNA was isolated and quantitative RT-PCR was performed to quantify the activation of S-phase genes. Values represent means; error bars are s.d. (n=3). An unpaired Student's t test was used to identify significant differences (*P<0.05) when compared with data from samples without torin1 treatment.

a

```
  1 MSGVVRSSPG SSQPPPPPPH HPPSSPVPVT STPVIPPIRR HLAFASTKPP FHPSDDYHRF NPSSLSNNND RSFVHGCGVV
 81 DREEDAVVVR SPSRKRKATM DMVVAPSNNG FTSSGFTNIP SSPCQTPRKG GRVNIKSKAK GNKSTPQTPI STNAGSPITL
161 TPSGSCRYDS SLGLLTKKFV NLIKQAKDGM LDLNKAAETL EVQKRRIYDI TNVLEGIDLI EKPFKNRILW KGVDACPGDE
241 DADVSVLQLQ AEIENLALEE QALDNQIRQT EERLRDLSEN EKNQKWLFVT EEDIKSLPGF QNQTLIAVKA PHGTTLEVPD
321 PDEAADHPQR RYRIILRSTM GPIDVYLVSE FEGKFEDTNG SGAAPPACLP IASSSGSTGH HDIEALTVDN PETAIVSHDH
401 PHPQPGDTSD LNYLQEQVGG MLKITPSDVE NDESDYWLLS NAEISMTDIW KTDSGIDWDY GIADVSTPPP GMGEIAPTAV
481 DSTPR
```

b

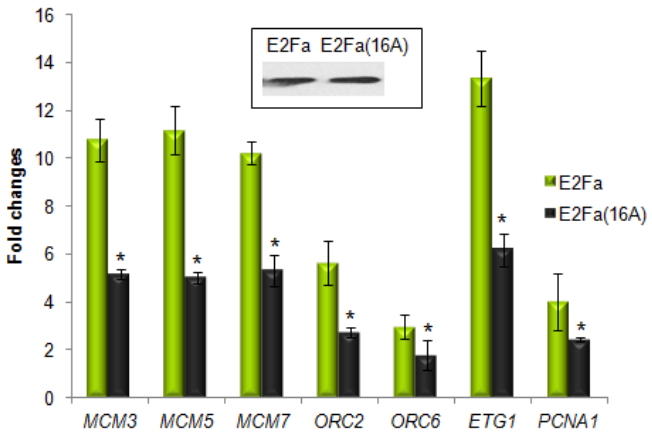

Supplementary Figure 20 | Putative TOR phosphorylation sites in E2Fa. a, The putative TOR phosphorylation sites were located in the N-terminal 80 residues of E2Fa. The 16 amino acids systematically tested by mutagenesis analyses (S or T to A) for TOR-dependent E2Fa activity in target gene activation were marked in red. **b,** The mutation of all 16 Ser/Thr residues (E2Fa (16A) significantly diminished E2Fa activity. E2Fa-HA or E2Fa (16A)-HA was transiently expressed in protoplasts for 4 h. Total RNA was isolated and quantitative RT-PCR was performed to quantify the activation of S-phase genes. Values represent means; error bars are s.d. (n=3). Unpaired Student's t test was used to identify significant differences (****P*<0.05) when compared with the data from E2Fa samples.

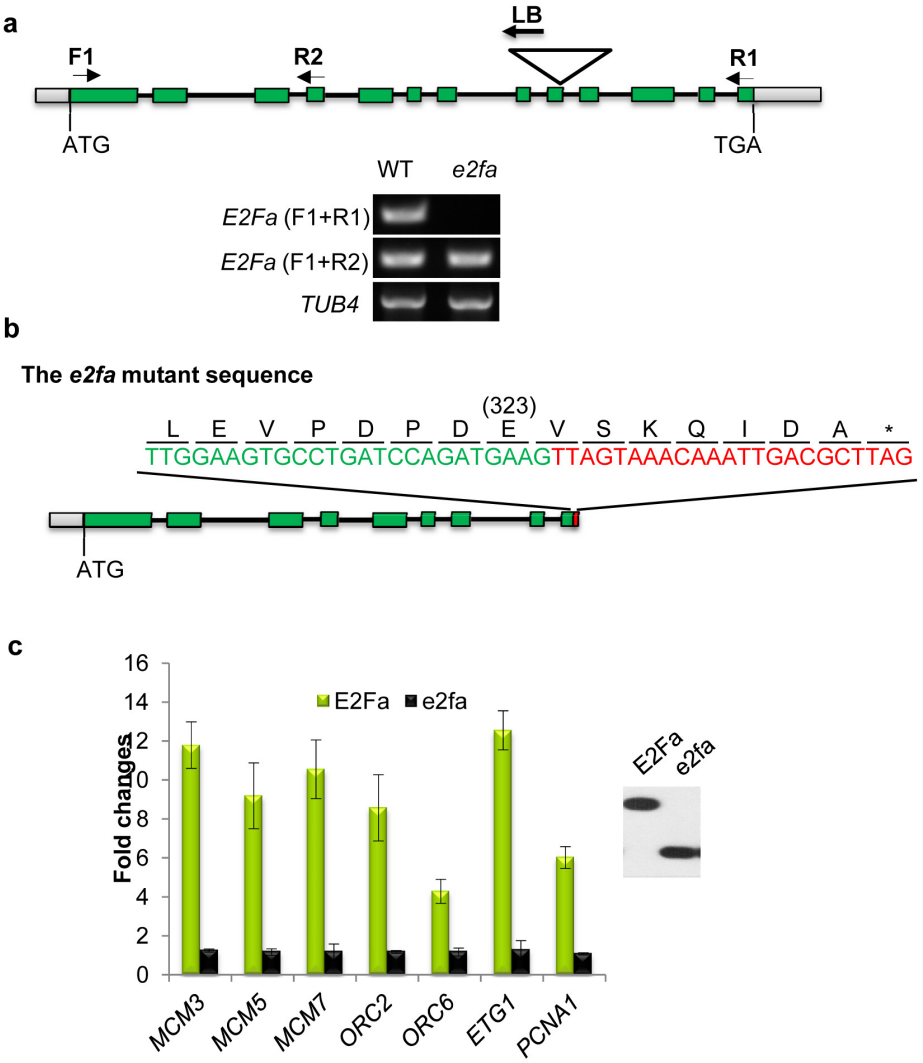

Supplementary Figure 21 | Molecular analyses of the *e2fa* mutant. a, T-DNA insertion in the *E2Fa* gene was in the 11th exon in the *WiscDsLox434F1* mutant line. Total RNA was isolated from 7-day-old seedlings. The upstream (F1+R2) but not the full-length *E2Fa* (F1+R1) transcript was detected in *e2fa* by RT-PCR. **b,** The *e2fa* mutant sequence. Green letters indicate the DNA sequence derived from *E2Fa*, and red letters indicate the DNA sequence derived from the T-DNA insertion. The residue E323 is the last amino acid from E2Fa. **c,** The truncated e2fa protein cannot activate S-phase target genes. E2Fa-HA or e2fa-HA was transiently expressed in protoplasts for 4 h. Total RNA was isolated and quantitative RT-PCR was performed to analyse the activation of S-phase genes. Values represent means; error bars are s.d. (n=3).

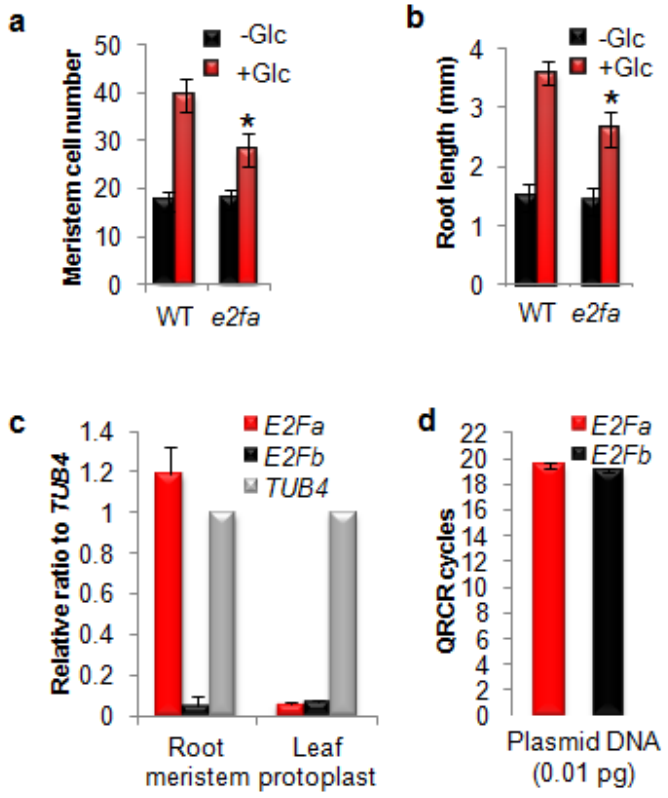

Supplementary Figure 22 | E2Fa plays a key role in the glucose promotion of root meristem activation and growth. a-b, Quantitative measurement of the root meristem cell number and root length in WT and *e2fa* seedlings. Seedlings at 3DAG were treated with 15 mM glucose (Glc) for 24 h. Values represent means; error bars are s.d. (n≥30). Unpaired Student's t test was used to identify significant differences (*P<0.05) when compared with the data from WT samples treated with glucose. **c-d,** Predominant expression of *E2Fa* in root meristems. Total RNA was isolated from root meristem tissues or leaf protoplasts. Quantitative RT-PCR was performed to analyse the relative expression level of *E2Fa*, *E2Fb* and *TUB4*. Comparable primer efficiency for *E2Fa* and *E2Fb* was confirmed by quantitative PCR using 0.01 pg plasmid DNA as templates. Values represent means; error bars are s.d. (n=3).

SUPPLEMENTARY TABLES

Supplementary Table 1 | Glucose-TOR target genes. The data in Supplementary Table 1 include both up-regulated (P value < 0.01; signal log2 ratio ≥1) and down-regulated (P value < 0.01; signal log2 ratio ≤ -1) glucose-TOR target genes, which are visualized in Fig. 4a, c and available as a Microsoft Excel file. Functional classification is based on Mapman[1]. Some genes appear in multiple classes.

Supplementary Table 2 | Novel glucose regulated genes. These genes are specifically defined in our experimental conditions, but not in prior studies using seedlings treated with glucose or sucrose, or 5-week-old leaves at low CO_2 conditions[6-8]. The data in Supplementary Table 2 is highlighted in Fig. 4a-d and available as a Microsoft Excel file. Functional classification is based on Mapman[1].

Functional categories	Gene count	Fold enrichment	P-value
Protein synthesis	109	1.5	1.1E-06
Cell cycle and DNA synthesis	105	1.5	5.3E-06
Protein folding	78	1.7	3.9E-06
Cell wall	60	2.2	4.4E-09
RNA synthesis	38	1.9	4.0E-05
Amino acid metabolism	31	2.4	4.0E-06
Nucleotide synthesis	29	3.2	1.8E-08
TCA and ETC	26	1.9	1.2E-03
Redox	19	1.7	7.0E-03
Glucosinolate synthesis	17	5.4	4.3E-09
Lignin synthesis	11	5.3	3.1E-06
Glycolysis	9	2.5	6.7E-03
S-assimilation	6	8.0	4.2E-05

Supplementary Table 3 | Over-represented functional categories up-regulated by glucose-TOR signalling. The genes were functionally classified using Mapman[1]. The enriched/over-represented fold changed is calculated as follows: (Number of Classified$_{input_set}$/ Number of total$_{input_set}$)/ (Number of Classified$_{reference_set}$/ Number of total$_{reference_set}$). The P-value is calculated in Excel using a hypergeometric distribution test.

Functional categories	Gene count	Fold enrichment	P-value
Protein degradation	96	1.3	2.2E-03
Development	44	1.5	3.3E-03
Lipid degradation	29	1.7	2.2E-03
Amino acid degradation	27	2.6	3.6E-06
CHO metabolism	25	2.5	1.8E-05
Redox	19	2.2	7.6E-04
Autophagy	7	7.6	1.8E-05
Biodegradation of Xenobiotics	5	4.0	5.8E-03
Glyoxylate cycle	4	8.7	7.1E-04

Supplementary Table 4 | Over-represented functional categories down-regulated by glucose-TOR signalling. Genes were functionally classified using Mapman[1]. The enriched/over-represented fold changed was calculated as follows: (Number of Classified$_{input_set}$/ Number of total$_{input_set}$)/ (Number of Classified$_{reference_set}$/ Number of total$_{reference_set}$). The P-value was calculated in Excel using a hypergeometric distribution test.

Supplementary Table 5 | Glucose-TOR target gene list (P value <0.01). The data in Supplementary Table 5 include both up- and down-regulated glucose-TOR target genes (P value < 0.01), which was used for hierarchical clustering analysis with cell cycle related genes[9] (Fig. 4e) and putative E2Fa target genes (Fig. 4f), and available as a Microsoft Excel file.

Supplementary Table 6 | Glucose-TOR target genes involved in cell cycle. The data in Supplementary Table 6 include glucose-TOR target genes (P value < 0.01) and the putative G1-, S-, G2- and M-phase genes[9]. The overlaps between glucose-TOR target genes and cell cycle genes are indicated with signal ratio > or < 0, presented in Fig. 4e, and available as a Microsoft Excel file.

Supplementary Table 7 | Putative E2Fa target genes. The 84 putative E2Fa target genes are defined by stringent overlap (Venn diagram in Supplementary Fig. 12) among *E2Fa* co-expression genes generated by Genevestigator (**www.genevestigator.com**), genes possessing putative E2Fa-binding motifs in the promoter regions[2], and genes up-regulated by E2Fa identified from seedlings that ectopically express E2Fa and DPa transcripiton factors driven either by the 35S constitutive promoter[2,3] or the DEX-inducible promotor[4]. The 84 putative E2Fa target genes were used for comparison with glucose-TOR target genes (Fig. 4f), and are available as a Microsoft Excel file. Genes used for qRT-PCR verification are highlighted.

Supplementary Table 8 | Primers used for qRT-PCR. F: forward; R: reverse

Name	AGI Number	Primers
E2FA	At2g36010	AGGCCAAAGGAAACAAGTCAACTCC
		TGCAGCTTTGTTTAGGTCCAGCATT
E2FB	At5g22220	GAGGAAAGCACCGAAAGAAACATGG
		TGACTTCGCCTACCTCTGATCGAA
TUB4	At5g44340	F: AGGGAAACGAAGACAGCAAG
		R: GCTCGCTAATCCTACCTTTGG
EIF4E	At3g13920	F: TCATAGATCTGGTCCTTGAAACC
		R: GGCAGTCTCTTCGTGCTGAC
IAA1	At4g14560	F: CACAGAGCTTCGTTTGGGATTACCC
		R: GCCATCCAACGATTTGTGTTTTTGC
IAA29	At4g32280	F: GGGAAAGAGGGTGACTGGCTACTTC
		R: TGGTCCGATTTGAACGCCTATCCTT
SAUR62	At1g29430	F: ACAAAGAGCAGCCCTCAAGA
		R: ACGGATCTTATCAGCCGTGT
ARR4	At1g10470	F: TTAGCCGTTGATGACAGTCTCGTTG
		R: CAGAGCACGCCATCCACTATCTACC
ARR7	At1g19050	F: CCGGTGGAGATTTGACTGTT
		R: ACTGCAAAGCCCTAGTTCCA
ARR16	At2g40670	F: TGCCTGGAATGACAGGTTTT
		R: TGAGCTCCACTCGCTAAACA
MCM3	At5g46280	F: CTTCGCCACAAGCGAGATTTTATCC
		R: TGGCTGCGTCACAAAATGACTG

MCM5	At2g07690	F: CAATTCGCCAGCCTTATATCCGAGT
		R: GGAGCGATCTTGGTGCAAATGTTC
MCM7	At4g02060	F: GCCGACGCTAATGGCAGATCTAA
		R: GCGGCGGAGAAAATTGAAACATATC
ORC2	At2g37560	F: TGGGTGGGGCGAGTAAGCGT
		R: AGGCCAAAGCCACACCTGAGC
ORC6	At1g26840	F: CGCCGCCACTAGGTTGCAGATTA
		R: ACAGCCAAATTGAACCGCCAATTC
CDC6	At2g29680	F: ATGCCTGCAATCGCCGGACC
		R: GGCAACACCACCGTCGCTGA
ETG1	At2g40550	F: CCCACGCCTCCATTGTCTTATCC
		R: GAACTGTGCGGCAATGTGATCATTC
PCNA1	At1g07370	F: CCTGATGCTGAGTACCACTCAATCG
		R: TGAGCACAATGTTAGCGGTTCCA

Supplementary Table 9 | Primers used for the *E2Fa* and *RPS6* constructs. F: forward; R: reverse.

Name	Primer sequence
E2Fa-F1	CGGGATCCATGTCCGGTGTCGTACGATC
E2Fa-R1	AAGGCCTTCTCGGGGTTGAGTCAACA
E2Fa-R2	TGCAGCTTTGTTTAGGTCCAGCATT
E2Fa-Δ1-R	AAGGCCTTCCTCCTACTTGCTCTTGCAA
E2Fa-Δ2-F	CGGGATCCATGCCATCAGGAAGTTGTCGTTATG

E2Fa-Δ4-F	**CGGGATCCATGGATCGGGAGGAAGATGCTG**
RPS6-F	**CATGCCATGGGAAAAGAGGATGATGTGAGGA**
RPS6-R	**AAGGCCTAGCAGCAACGGGTTTAGC**

Supplementary Table 10 | Primers used E2Fa mutagenesis analyses F: forward; R: reverse

Name	**Primers**
E2Fa(7, 8AA)	**F: CGGTGTCGTACGAGCTGCTCCCGGTTCTTCTC**
	R:GAGAAGAACCGGGAGCAGCTCGTACGACACCG
E2Fa(11, 12AA)	**F: ATCTTCTCCCGGTGCTGCTCAGCCGCCACCGC**
	R: GCGGTGGCGGCTGAGCAGCACCGGGAGAAGAT
E2Fa(24, 25AA)	**F: CACCATCCACCGGCAGCTCCGGTTCCGGTTA**
	R:TAACCGGAACCGGAGCTGCCGGTGGATGGTGC
E2Fa(30, 31, 32AA)	**F: TCCGGTTCCGGTTGCAGCTGCGCCGGTTATAC**
	R: GTATAACCGGCGCAGCTGCAACCGGAACCGGA
E2Fa(46, 47AA)	**F: CTTAGCTTTCGCCGCAGCAAAACCTCCGTTTC**
	R: AAACGGAGGTTTTGCTGCGGCGAAAGCTAAG
E2Fa(54A)	**F: TCCGTTTCATCCTGCCGATGATTACCATC**
	R: GATGGTAATCATCGGCAGGATGAAACGGA
E2Fa(63, 64, 66AAA)	**F: ATTTAACCCTGCTGCGCTCGCTAATAATA**
	R: TATTATTAGCGAGCGCAGCAGGGTTAAAT
E2Fa(72A)	**F: TAATAACGACAGGGCCTTCGTTCATGGTT**
	R: AACCATGAACGAAGGCCCTGTCGTTATTA

Supplementary Table 11 | Primers used for ChIP-qPCR assays. F: forward; R: reverse; P: promoter; G: gene body

Name	**Primer sequence**
CAB1-G-F	**TCCCTGAGCTTTTGGCTAGA**
CAB1-G-R	**AACGGCTCCCATCAAAATAA**
MCM5-P-F	**AGAAAGAAAGACCCAATAACCAAC**
MCM5-P-R	**TCTAAACGAAGAGAGAGAGTGGG**
MCM5-G-F	**CTACAGGAGAATCCGGAGGT**
MCM5-G-R	**ACGAAGCTTGGAAAATGCTG**
ETG1-P-F	**GTTGGAAGTTGGAGAATGGG**
ETG1-P-R	**CGAATTAAGGGCAATGTCAA**
ETG1-G-F	**AAAACAGGGAAAAGCGTGTG**
ETG1-G-R	**CCATTACGCCCAGCTTCTAA**

SUPPLEMENTARY METHODS

Antibodies and protein blot analysis. Phospho-p70 S6 Kinase (p-Thr389) polyclonal antibody (Cell Signalling) was used to detect TOR kinase phosphorylation of p-T449 in *Arabidopsis* S6K1. HA- or FLAG-tagged proteins were detected by anti-HA (Roche) or anti-FLAG (Sigma) monoclonal antibodies using standard techniques. Polyclonal *Arabidopsis* TOR antibody was generated as described[10].

Plasmid constructs. The construct of S6K1-FLAG for protoplast transient expression has been previously described[10]. The construct of 4E-BP1-6HIS was from Addgene. For constructs of *E2fa* (*At2g36010*) and its truncated variants (Δ1, amino acids 1-420; Δ2, amino acids 162-420; Δ3, amino acids 162-485; Δ4, amino acids 81-420; *e2fa*, amino acids 1-323) or RPS6B (amino acids 150-249), the coding regions were amplified from *Arabidopsis* Col-0 complementary DNA, then fused to the HA tag and cloned between the *35S*-drived promoter and *NOS* terminator[11,12] for protoplast transient expression, or fused to the 6HIS tag in the pet14b plasmid (Addgene) for *E. coli* expression and purification as in vitro TOR kinase or S6K1 kinase substrates. All primers used are listed in Supplementary Table 9. The E2Fa (16A) mutant were generated by PCR-based site-specific mutagenesis[10] and primers used are listed in Supplementary Table 10.

E2Fa-6HIS, 4E-BP1-6HIS and RPS6B-6HIS protein expression and purification. Transfected *E. coli* cells in 500 ml LB medium with ampicillin (100 μg/ml) were grown at 37°C until A_{600} = 0.7. The cell culture was then cooled to 18°C before IPTG was added to a final concentration of 0.3 mM, and cells were incubated for an additional 12 h at 18°C to induce the expression of 6HIS tagged protein. Cells were harvested by centrifugation at 4,000xg for 20 min

and stored at -80°C. The 6HIS tagged protein was purified using Ni-NTA agarose (Qiagen) under native condition according to the manufacturer's instructions. Briefly, using the Qproteome Bacterial Protein Prep Kit (Qiagen) with 1X cocktail inhibitors, cells were lysed and then incubated for 30 min on ice. The lysed solution was centrifuged at 10,000xg for 30 min and the supernatant was incubated with 100 µl Ni-NTA agarose for 2 h at 4°C. The Ni-NTA agarose was washed 3 times with washing buffer (50 mM NaH_2PO_4, pH 8.0, 300 mM NaCl, 40 mM imidazole), and the 6HIS fusion protein was eluted with 3 ml elution buffer (50 mM NaH_2PO_4, pH 8.0, 300 mM NaCl, 250 mM imidazole) and concentrated by Amicon Ultra filter (Millpore).

In vitro TOR protein kinase assays. For in vitro TOR kinase assays, seedlings were lysed in 500 µl immunoprecipitation (IP) buffer (400 mM HEPES, pH 7.4, 2 mM EDTA, 10 mM pyrophosphate, 10 mM glycerol phosphate, 0.3% CHAPS and 1X cocktail inhibitors [Roche]). To immunoprecipitate endogenous TOR, protein extracts were incubated with anti-TOR antibody at 4°C for 2 h, and additional 1 h after adding 15 µl protein G sepharose beads (GE healthcare). The immunoprecipitated TOR kinase was washed twice with low salt wash buffer (400 mM HEPES, pH 7.4, 150 mM NaCl, 2 mM EDTA, 10 mM pyrophosphate, 10 mM glycerol phosphate, 0.3% CHAPS) and once with kinase wash buffer (25 mM HEPES, pH 7.4, 20 mM KCl). Kinase reaction was performed for 30 min in 30 µl kinase buffer (25 mM HEPES, pH 7.4, 50 mM KCl, 10 mM $MgCl_2$, 10 µM cold ATP, 2 µCi [γ-^{32}P] ATP and 1 µg E2Fa-6HIS or 4E-BP1-6HIS substrates without/with torin1 (1µM) or staurosporine (1µM) at 25°C. The reaction was stopped by adding SDS-PAGE loading buffer. After separation on 10% SDS-PAGE and subsequent gel drying, radiolabelled E2Fa-6HIS or 4E-BP1-6HIS was detected on the dried gel by the Typhoon imaging system (GE Healthcare).

In vitro S6K1 protein kinase assays. In vitro S6K1 kinase assay was performed as described[13]. Protoplasts (10^5) were transfected with 50 µg S6K1-HA and incubated for 6 h in 5 ml of mannitol (0.5 M) and KCl (20 mM) buffer (4 mM MES, pH 5.7) in Petri dish (100 mm x 20 mm). The collected protoplasts were lysed in 500 µl immunoprecipitation (IP) buffer (50 mM Tris-HCl, pH 7.5, 150 mM NaCl, 5 mM EDTA, 1% Triton X-100, 1 mM DTT, 1 mM $NaVO_3$, 5 mM NaF and 1X cocktail inhibitors [Roche]). To immunoprecipitate S6K1-HA, protein extracts were incubated with anti-HA antibody at 4°C for 2 h, and additional 1 h after adding 15 µl protein G sepharose beads (GE healthcare). The immunoprecipitated S6K1 kinase was washed 3 times with IP buffer. Kinase reaction was performed for 30 min in 30 µl kinase buffer (20 mM HEPES, pH 7.4, 125 mM NaCl, 10 mM $MgCl_2$, 5 mM $MnCl_2$, 10 µM cold ATP, 2 µCi [γ-^{32}P] ATP and 1µg RPS6B-6HIS substrates without/with torin1 (1µM) or staurosporine (1µM) at 25°C. The reaction was stopped by adding SDS-PAGE loading buffer. After separation on 10% SDS-PAGE and subsequent gel drying, radiolabelled S6K1-6HIS was detected on the dried gel by the Typhoon imaging system (GE Healthcare).

Co-immunoprecipitation (Co-IP) for the E2Fa-TOR interaction assay. Protoplasts (5 X 10^5) were transformed with 25 µg E2Fa-FLAG and incubated in 5 ml of mannitol (0.5 M) and KCl (20 mM) buffer (4 mM MES, pH 5.7) in Petri dishes (100 mm x 20 mm, 10^5 cells/each) for 4 hours. Collected protoplasts were lysed in 500 µl Co-IP buffer (400 mM HEPES pH 7.4, 2 mM EDTA, 10 mM pyrophosphate, 10 mM glycerol phosphate, 0.3% CHAPS and 1X cocktail inhibitors [Roche]). To immunoprecipitate TOR, protein extracts were incubated without/with anti-Flag antibody at 4°C for 2 h, and additional 2 h after adding 15 µl protein G sepharose beads

(GE healthcare). The immunoprecipitated proteins were washed four times with low salt wash buffer (400 mM HEPES pH 7.4, 150 mM NaCl, 2 mM EDTA, 10 mM pyrophosphate, 10 mM glycerol phosphate, 0.3% CHAPS) before SDS-PAGE separation and protein blot analyses.

Chromatin immunoprecipitation (ChIP) assays. Protoplasts (5 X 10^5) were transformed with 25 μg E2Fa-HA or E2Fa-Δ4-HA construct and incubated in 5 ml of mannitol (0.5 M) and KCl (20 mM) buffer (4 mM MES, pH 5.7) in Petri dishes (100 mm x 20 mm, 10^5 cells/each) for 4 h. For experiments analysing the effect of rapamycin, and torin1, protoplasts were pretreated with rapamycin (1 μM), or torin1 (100 nM) for 1 h before E2Fa transfection. Cells were then crosslinked by 1% formaldehyde for 20 min and quenched by glycine (0.2 M) for 5 min. Nuclei were extracted freshly as described previously[14] and the rest of ChIP steps was then performed essentially as described in the Pikaard lab protocol (http://sites.bio.indiana.edu/~pikaardlab/Protocols%20page.html) with some modifications. Bioruptor (Diagenode) was used for chromatin sonication. DNA was eluted by 1% SDS and 0.1 M $NaHCO_3$ at 65 ^oC for overnight. Anti-HA antibody (Roche) was used in this study. All the qPCR primers showed similar efficiency tested with the input DNA as controls. The final relative enrichment fold changes were calculated by normalizing % input of each primer pair against the control gene (*CAB1*), which is not an E2Fa target gene. Values are mean with error bars derived from two independent biological replicates. All primers used are listed in Supplementary Table 11.

Microarray analysis. Three-day-old quiescent WT and *tor* seedlings were treated without or with glucose (15 mM) for 2 h. Total RNA was extracted using RNeasy Plant Mini kit (Qiagen)

according to the manufacturer's protocol. Total RNA (4 μg) was converted to cDNA, and amplified and biotinylated using the BioArray Highyield RNA transcript labeling kit (Enzo) according to the manufacturer's instructions. The cRNAs were fragmented in fragmentation buffer (40 mM Tris-Acetate, pH 8.1, 100 mM KOAc, 30 mM MgOAc), 94 ^{o}C for 35 minutes. Hybridization to *Arabidopsis* ATH1 GeneChip arrays (Affymetrix) and scanning were conducted by the Advanced Genomics and Genetics Core microarray facility of Joslin Diabetes Centre.

Quality assessment. Before analysing for expression differences, the quality of raw arrays were assessed with the aid of the BioConductor packages arrayQualityMetrics[15], simpleaffy[16], affyPLM[17], and Harshlight[18]. Harshlight was used to assess for possible physical defects of the arrays and/or hybridization problems. The other BioConductor packages provide an array of metrics, which were used in making a judgment of the quality of the microarray chips.

Expression analysis. Expression analysis was performed using both RMA[19,20] and dChip[21] in FlexArray 1.6.1[22]. Affymetrix CEL files were imported into FlexArray, and both dChip (subtract MM from PM) and RMA (correct background and normalize) analyses were performed. Each analysis was followed by cyber-T (window size 101, Confidence ratio of 10) to statistically test for differences in expression. Results from both the dChip and RMA analysis were exported out of FlexArray and into Excel. In Excel, the RMA and dChip analysis were separately filtered in two or three steps depending on the analysis. The first step eliminated genes with a p-value of less than 0.01 and was done in all the analyses. The second step, not employed in generating gene lists for comparison with cell cycle data and E2Fa target data (Fig. 4e and f; and Supplementary Table 5), eliminated genes with a signal log ratio of between -0.99 and 0.99. A

final step, done in all analyses, eliminated genes not present in both the RMA and dChip analysis after the first or both of the two above filters had been applied. The resulting gene list (Supplementary Table 5) used for cell cycle comparison and E2Fa targeted gene comparison contains genes with a p-value of 0.01 or less, and were present in both the RMA and dChip analysis (Fig. 4e, f). The resulting gene list (Supplementary Table 1) used for comparison with glucose, sucrose and low CO_2 data (Fig. 4a, c) or for functional classification (Fig. 4b, d) contains genes with a p-value of 0.01 or less, as well as a two-fold or more increase or decrease in expression, and were present in both the RMA and dChip analysis.

Generation of glucose regulated gene list. The expression analysis described above was used to analyse gene expression changes between untreated wild-type plants (wt-ctr) and glucose treated wild-type plants (wt-glc), or untreated *tor* plants (*tor*-ctr) and glucose treated *tor* plants (*tor*-glc). The set of genes resulting from this analyse was used for comparison with all public microarray data. When the signal log ratio cutoff was used, this set of genes contained 2368 genes (Supplementary Table 1). When the signal log ratio cutoff was not used, this set contained 4778 genes (Supplementary Table 5). Estradiol itself and the inducible system did not result in any significant changes in gene expression in microarray analysis, which was confirmed using the estradiol-inducible-GUS transgenic lines (Data not shown).

Analyses of public microarray data. Analyses of all publically available microarray data used in Fig. 4 were accomplished as described above in the Expression Analysis section. The signal

log2 ratio filter was used for Figure 4a and c, and Supplementary Table 1. The list of cell cycle genes was taken from Supplementary Table 12 in Menges et al., 2003[9].

Clustering analyses. Gene lists resulting from microarray analyses were imported into Cluster 3.0[23] where hierarchical agglomerative clustering was performed. The results were visualized in Java TreeView[24]. Figure 4a and c were generated using absolute correlation (uncentered) as the distance metric with centroid linkage, and correlation (uncentered) was used as the distance metric with single linkage to generate Figure 4e.

Functional classification. Functional classification of glucose-TOR regulated genes was carried out by Mapman[1] and BAR[25] (http://bar.utoronto.ca). The results were sorted in Excel to draw the pie charts for Fig. 4b and d. Specifically, the cell cycle & DNA synthesis category contains both cell cycle, cell division, and DNA synthesis genes; the metabolism category contains genes involved in primary and secondary metabolic pathways but not specifically classified in Fig. 4b and d (See Supplementary Table1 for details).

E2Fa co-expression analysis. E2Fa co-expression analysis was carried out by Genevestigator (www.genevestigator.com) using the perturbations option. The Pearson correlation coefficient was used as a measure of similarity between gene expression patterns. The score is calculated on log2-scaled expression data that is processed from the Genevestigator database.

Definition of putative E2Fa target genes. E2Fa co-expression genes were generated as described above. E2Fa_binding_motif containing genes were identified by Naouar et al., 2009[2]. E2Fa up-regulated genes were identified from three microarray data sets using seedlings that ectopically express E2Fa and DPa transcription factors driven either by the 35S constitutive promoter[2,3] or the DEX-inducible promoter[4] (6 h treatment). The putative E2Fa target genes presented in all of these three categories were selected and used for comparison with glucose-TOR target genes (Fig. 4f). See Supplementary Table 7 for complete gene sets.

SUPPLEMENTARY REFERENCES

1. Thimm, O. *et al.* MAPMAN: a user-driven tool to display genomics data sets onto diagrams of metabolic pathways and other biological processes. *Plant J* **37**, 914-939 (2004).

2. Naouar, N. *et al.* Quantitative RNA expression analysis with Affymetrix Tiling 1.0R arrays identifies new E2F target genes. *Plant J* **57**, 184-194 (2009).

3. Vandepoele, K. *et al.* Genome-wide identification of potential plant E2F target genes. *Plant Physiol* **139**, 316-328 (2005).

4. de Jager, S. M. *et al.* Dissecting regulatory pathways of G1/S control in Arabidopsis: common and distinct targets of CYCD3;1, E2Fa and E2Fc. *Plant Mol Biol* **71**, 345-365 (2009).

5. Oliveros, J.C. VENNY. An interactive tool for comparing lists with Venn Diagrams (2007). http://bioinfogp.cnb.csic.es/tools/venny/index.html.

6. Li, Y. *et al.* Establishing glucose- and ABA-regulated transcription networks in Arabidopsis by microarray analysis and promoter classification using a Relevance Vector Machine. *Genome Res* **16**, 414-427 (2006).

7. Blasing, O. E. *et al.* Sugars and circadian regulation make major contributions to the global regulation of diurnal gene expression in Arabidopsis. *Plant Cell* **17**, 3257-3281 (2005).

8. Gonzali, S. *et al.* Identification of sugar-modulated genes and evidence for in vivo sugar sensing in Arabidopsis. *J Plant Res* **119**, 115-123 (2006).

9. Menges, M., Hennig, L., Gruissem, W. & Murray, J. A. Genome-wide gene expression in an Arabidopsis cell suspension. *Plant Mol Biol* **53**, 423-442 (2003).

10. Xiong, Y. & Sheen, J. Rapamycin and glucose-target of rapamycin (TOR) protein signaling in plants. *J Biol Chem* **287**, 2836-2842 (2012).

11. Kovtun, Y., Chiu, W. L., Zeng, W. & Sheen, J. Suppression of auxin signal transduction by a MAPK cascade in higher plants. *Nature* **395**, 716-720 (1998).

12. Hwang, I. & Sheen, J. Two-component circuitry in Arabidopsis cytokinin signal transduction. *Nature* **413**, 383-389 (2001).

13. Mahfouz, M. M., Kim, S., Delauney, A. J. & Verma, D. P. Arabidopsis TARGET OF RAPAMYCIN interacts with RAPTOR, which regulates the activity of S6 kinase in response to osmotic stress signals. *Plant Cell* **18**, 477-490 (2006).

14. Sheen, J. Protein phosphatase activity is required for light-inducible gene expression in maize. *EMBO J* **12**, 3497-3505 (1993).

15. Kauffmann, A., Gentleman, R. & Huber, W. arrayQualityMetrics--a bioconductor package for quality assessment of microarray data. *Bioinformatics* **25**, 415-416 (2009).

16. Wilson, C. L. & Miller, C. J. Simpleaffy: a BioConductor package for Affymetrix Quality Control and data analysis. *Bioinformatics* **21**, 3683-3685 (2005).

17. Jones, L. *et al.* Assessment of the relationship between pre-chip and post-chip quality measures for Affymetrix GeneChip expression data. *BMC Bioinformatics* **7**, 211 (2006).

18. Suarez-Farinas, M., Pellegrino, M., Wittkowski, K. M. & Magnasco, M. O. Harshlight: a "corrective make-up" program for microarray chips. *BMC Bioinformatics* **6**, 294 (2005).

19. Irizarry, R. A. *et al.* Summaries of Affymetrix GeneChip probe level data. *Nucleic Acids Res* **31**, e15 (2003).

20. Irizarry, R. A. *et al.* Exploration, normalization, and summaries of high density oligonucleotide array probe level data. *Biostatistics* **4**, 249-264 (2003).

21. Li, C. & Hung Wong, W. Model-based analysis of oligonucleotide arrays: model validation, design issues and standard error application. *Genome Biol* **2**, (2001).

22. Michal Blazejczyk, M. M., Robert Nadon FlexArray: A statistical data analysis software for gene expression microarrays. *Genome Quebec* (2007).

23. de Hoon, M. J., Imoto, S., Nolan, J. & Miyano, S. Open source clustering software. *Bioinformatics* **20**, 1453-1454 (2004).

24. Saldanha, A. J. Java Treeview--extensible visualization of microarray data. *Bioinformatics* **20**, 3246-3248 (2004).

25. Toufighi, K., Brady, S. M., Austin, R., Ly, E. & Provart, N. J. The Botany Array Resource: e-Northerns, Expression Angling, and promoter analyses. *Plant J* **43**, 153-163 (2005).